



APPLICATION OF DATA VISUALIZATION INTERACTION TECHNOLOGY IN AEROSPACE DATA PROCESSING

JIA LIN^{*}, BIGENG ZHENG[†] AND ZHIJIAN CHEN[‡]

Abstract. A visualization and interactive network topology model are studied based on real-time features generated during spaceflight. Start by establishing a consistent set of data and logical interaction interfaces. This paper presents a method of scenario model construction and application programming based on virtual reality technology. The scene elements are extracted into two types of primitives, namely logical type and simulated object type. This provides a unified architecture for the editing and processing of graphic elements. This system can realize the automatic creation of the scene. Then the point cloud data obtained by sparse reconstruction of SFM is reconstructed to the Poisson surface. You get a dense, uniform grid. Experiments show that the proposed algorithm can realize the 3D reconstruction of non-cooperative objects. The spatial feature points obtained in the spatial positioning of non-cooperative objects can provide necessary technical support for its orbit positioning. The model can quickly generate new model scenario pages according to the characteristics of the task. This method changes the display mode, which can only be static or limited dynamic before. It has also improved the efficiency of space mission preparation.

Key words: Space mission; Pixel; Visual interaction; Topology modeling; Three-dimensional reconstruction; Motion recovery structure (SFM)

1. Introduction. China's aviation technology innovation has grown by leaps and bounds to adapt to the fierce competition in space technology. China has completed several important space science and technology projects. Overall, it shows the development trend of multi-region, multi-model, multi-region and intensive firing. This has led to higher real-time demands across disciplines. It includes fast preparation, binding, switching, multiple presentations, and dynamic command and support scene construction. Traditional commercial applications such as space command and surveillance are a "waterfall" development process. Software requirements are based on user requirements. Then write a software requirements document. Then the software is designed, coded, tested and maintained. Due to the significant differences between the various types of spacecrafts, there is no single standard. Business systems software tends to be highly personalized. It is challenging to realize the repeated utilization of several tasks. Due to the lack of reusable software and efficient auxiliary methods, the development efficiency of the system is very low, and it isn't easy to meet the new development requirements.

Currently, the widely used network model construction technology of visualization software can be roughly divided into two categories: the personalized design based on interactive graphics. Put the image class into the program. However, this technology is more complicated, and the development time is relatively long. The number of codes increases geometrically. This is unfavorable to the expansion and maintenance of the software. One is a single development based on QtUiloader. This wraps the chart as a dynamic library that frames can access. It uses the "skeleton + plug-in" function in hot-swap mode. It reduces the difficulty of research and development and saves time. This approach reduces the maintenance complexity of the system. However, the industry has not yet established a universal 3D visual application model. Existing model-building methods are rarely applied. It only works for his business activities. This method has poor support for new devices, tasks, and models.

Construction from Motion (SFM) is a 3D reconstruction technique based on multi-frame images. Many foreign experts on this issue have done a lot of work. Literature [1] uses SFM technology for 3D reconstruction and develops a 3D automatic reconstruction system. Beam adjustment (BA) is an essential algorithm for SFM

^{*}School of Artificial Intelligence, Zhuhai City Polytechnic, Zhuhai 519090, China

[†]School of Electronic Information Engineering, Jingchu University of Technology, Jingmen 448000, China (Corresponding authors, 16826033@qq.com)

[‡]School of Microelectronics, South China University of Technology, Guangzhou, 511442 China

optimization. The point cloud data was obtained by minimizing the effect of repeated projections by the LM (Levenberg-Marquardt) method. Aiming at the problem that the current large amount of data is not suitable for large-scale reconstruction; some scholars intend to introduce a method based on sparse beam correction [2]. It reduces the size and complexity of operations. The dense point cloud is obtained using CMVS/PMVS (Clustering views Multi-View Stereo / Patch-based Multi-View Stereo) algorithm based on sparse point cloud reconstruction. The final 3D reconstruction results are satisfactory [3]. There are also many domestic research results. Literature [4] has conducted in-depth research on the fast calibration, fast image matching and fast and accurate basic matrix calculation required by the system in the 3D reconstruction of space non-cooperative targets. Literature [5] uses the imaging timing of continuous images as iterative prior information and uses improved SFM for 3D reconstruction. Literature [6] researched 3D reconstruction for CMVS/PMVS algorithm. Experimental results prove that this method is very effective in outdoor reconstruction. Based on the 3D reconstruction algorithm based on the brightness and darkness of a single frame image to restore the shape, Literature [7] proposed an infrared-self-shadow reconstruction (IR-SFS) method using external radiation and its radiation for 3D reconstruction. The overall effect has been significantly improved.

This paper presents a method of constructing a network model based on visual interaction. Develop interactive data and logic interfaces. This paper presents a method of scenario model construction and application programming based on virtual reality technology. The scene elements are extracted into two graph units, namely logical and analog shape graph units, and the corresponding algorithms are constructed. The system has the function of judging and processing the bundling parameters. You can quickly create scene pages like decision trees, flow charts, relationship diagrams, dynamic pipeline diagrams, device diagrams, etc. The new number, task scene drags, visual topology modeling, graphics drawing, interactive display, and other functions are realized. The SFM algorithm is applied to the sparse point cloud reconstruction of non-cooperative objects. The CMVS/PMVS method reconstructs the dense point cloud data. At the same time, this project will also use Poisson reconstruction technology to improve the existing defects, such as non-uniform distribution and voids in the dense point cloud. Users can get a clear, intuitive view of non-cooperative targets. It realizes the function of space observation for ordinary users.

2. Development of network model construction system for visual interaction.

2.1. Network model structure of visual interaction. The visual architecture of "platform + plug-in" and "common + feature" is used to model the network topology. A set of web page editing systems is designed based on QtUiLoader. According to the different functions, the visual topology modeling system is divided into basic support layer, basic resource layer, basic service layer, platform interface layer, element component library and function application layer. A specific architecture diagram is shown in Figure 2.1.

The foundation support layer is the primary operating environment and supporting condition of the whole system. The focus is the self-developed operating system, hardware terminal, lightweight database, lightweight database, and Qt development platform.

The primary resource layer is the base load resource of the system. It is a vital resource investment. It provides image, video, and file resources for the system, such as device connection diagrams, cloud diagrams, geographic information resources, video monitoring resources, task introduction, personnel information, and task documents.

The underlying service layer is a platform-level function that implements the entire system. It is a general resource extraction for each component. Its content mainly includes a display filtering service, graphics cache service, display layout service, component management service, dynamic rendering service, UI interactive processing service, drawing board, annotation function, color palette, geometric transformation, data subscription, data cache, data processing, protocol management, analog pixel engine, logic pixel engine, configuration saving, task loading and other functions. The platform interface layer proposes a user-oriented software development method. It is a conduit between the whole system and the outside world. The primary interfaces are Drawing, data, control, and recording interfaces.

The functional application layer realizes a higher level of human-machine dialogue. It includes screen editing, artboard drawing, meta-loading, data modeling, screen organization and other functions.

The primitive component library extends the software at the component level. Perform maintenance work as required. In terms of types, it can be divided into quasi-object elements, logical elements, brush, graph, etc.

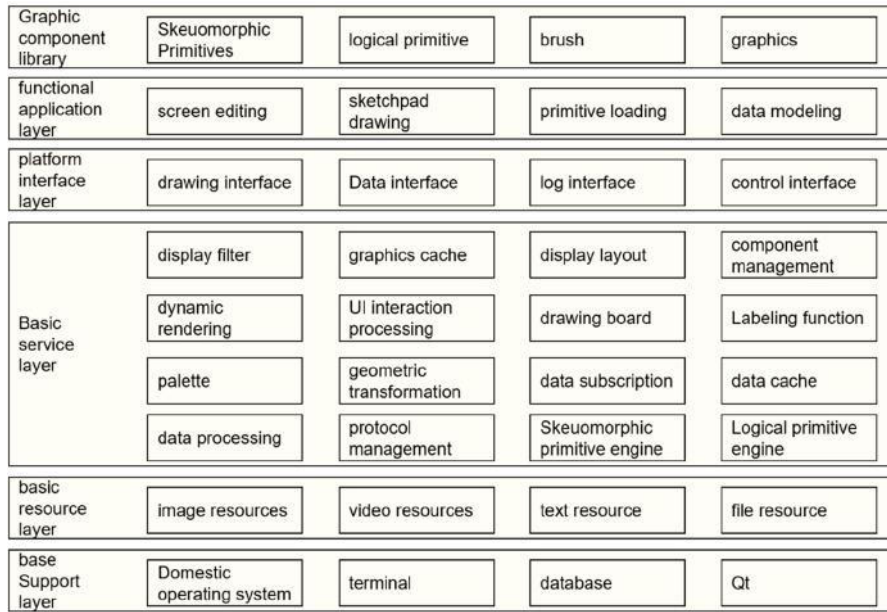


Fig. 2.1: Visual topology modeling system framework.

2.2. "Plug-in" function in the spatial model. In space operation, multiple components' states are often interrelated. A common approach is establishing a "number" or "status" parameter. The central computer data processing service generates the virtual parameter data. Commercial software orders virtual parameters for status presentations are needed. This approach applies to new equipment, models, tasks, and systems. Creating virtual parameters is not suitable for system expansion and state maintenance. The system design of the component connection mechanism only needs to set the correlation of components when the web page is set up. Setting the mode of operation allows the relevant state process to be performed. It is also extended to analog graphic elements and logical graphic elements. The consistency of the system is ensured at the data level. The analogs and logical primitives in the primitive's widget library are inherited from the QtUiLoader interface. In the case of no secondary development, components and layouts can be directly loaded into the business software to achieve the same interface of the business software. The construction of the primitive component is shown in Figure 2.2.

The primitives are inherited from the QtUiLoader. It can be mounted on the frame. The interface of receiving data, subscribing status and disclosing status is realized in this module. Use callback methods to complete data and state processing in the current part.

2.3. Flow chart of the visual interactive modeling system. This system is used to design the visual model of the network for different working types and models. They are modeling based on new model tasks and modeling based on historical tasks. Existing working model resources of the same type can be built on top of a historical working model. Only incremental changes are required [8]. The process of the visual topology model is shown in Figure 2.3.

First, the system tasks are classified and compared with the historical tasks in the system. If the match is successful, the historical task is directly loaded. It includes: setting page layout files, task history parameter data, task history theory data, etc. You can make incremental changes and add pages based on historical work. This would significantly reduce the preparation for such missions [9]. If the match is unsuccessful, new task information needs to be entered. The main contents include task name, task code, task parameters, task theory data, task menu structure, etc. After the dialogue between two people, arrange the webpage requirements and set up a new webpage according to the matching results and work requirements.

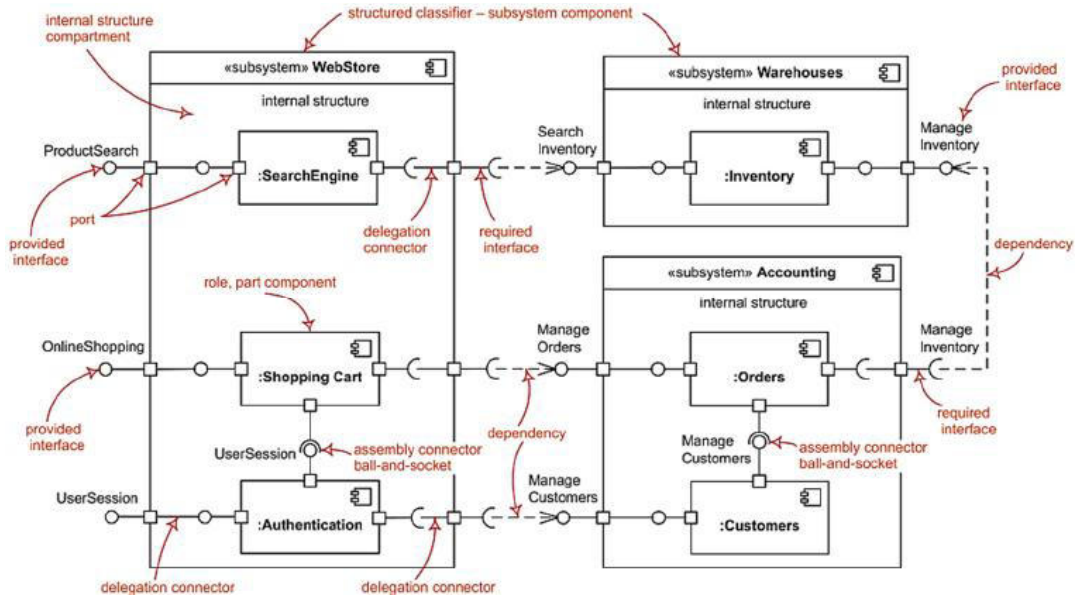


Fig. 2.2: Structure diagram of the element component.

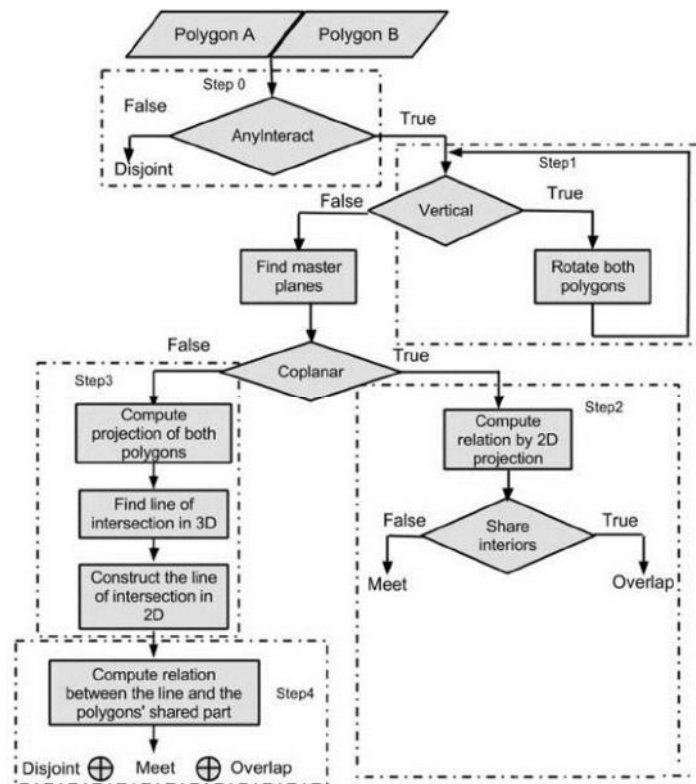


Fig. 2.3: Flowchart of visual topology modeling.

Secondly, the graphics meta component is initialized. Update the original component list and present the available information to the user. Create a new empty page. Parse the element requirements on the task page. Select the original component and drag it to the empty page [10]. Configure the graphic element style and structure layout. Repeat the previous steps until all graphic elements on the page are filled. Connect the corresponding graph nodes—Configure graphic element associations. Set up logical rules and simulate the behavior effects of objects according to the categories of graphic elements.

Finally, the graphics metadata source is configured, and whether the configuration is correct will be automatically judged. Save the web Settings to the local file when the settings are finished. It is used to load commercial software.

3. System implementation. According to the concept of "platform + plug-in," a visualization system of a 3D network model is developed. A series of graphic component libraries are designed for the control platform.

3.1. Build a primary model development platform. Firstly, the basic abstracting and extracting business and interface functions are completed from the architecture. The system is based on the Qt designer source code. It is a successor to the Qt localized visual operation interface. Provide user interface file management, editing, page layout, component management, property management and other essential functions. Implement filtering, caching, data subscription, task loading, exceptional attribute management and other functions [11]. The loading framework of logical elements and simulative elements is given. It can carry new symbols and added work management functions—the ability to load a working tree architecture. Build a primary model development platform. Establishing a basic modeling platform cannot realize all the system's functions but only provides the program object-oriented component library and primary data loading platform. In this process, you must enter the task information, real-time data resource configuration information, and historical data resource information in advance. A task configurator must be used to perform related functions—button wake-up function set on the platform.

3.2. Task Resource Configuration Tool. A resource setting tool that must perform work to set primary data. This tool can handle the database directly. It maintains and manages the database. The task resource configuration tool can manage all the work. Includes basic Settings for adding, viewing, modifying, and more. The job contains the job name, code, and description information. Manage all the real-time analysis data in the system [12]. Convert live data to subscription data. Provide ordering information for the component, including real-time and historical data. A parallel editing algorithm based on multiple nodes is proposed. This tool can update configuration information to a network database. Online database information can be brought to the local area.

3.3. Creation of graphics meta component. This paper completed the system design after the basic model construction and task resource allocation. You need to create a database of graphics metal parts for this article. The graph elements are divided into two types, namely logical graph elements and quasi-object graph elements. The logical graph elements include a decision tree, flow diagram, relationship diagram, dynamic pipeline diagram, equipment diagram and process diagram [13]. The simulated object elements include 14 elements, such as a switch, button, status light, pipeline, line, network equipment, telemetry equipment, external measurement equipment, code table, storage tank, curve chart, line chart, bar chart, pie chart, etc. One of the logical primitives represents the topology composition relationship. Various logical relationships are realized by configuring the elements of logical primitives according to certain logical relationships. The pseudo-object element reflects the connection between the pipe and the device. Lines connect and configure simulated elements through pipes—incremental updates to component libraries based on task requirements [14]. The relevant statistics listed in Table 3.1 are based on a one-person operation with 500 web pages per task. The modeling platform developed based on the visualization application topology modeling method significantly improved the preparation time of the single task and single page configuration. The operator is becoming more and more proficient. Its application effect will also be better.

4. Space data processing algorithm.

4.1. Sparse point cloud reconstruction. The SFM algorithm is essentially the projection matrix of the camera. The algorithm uses the relevant positioning information of the camera. 3D information about objects

Table 3.1: Efficiency comparison of modeling methods.

	Task preparation time /min	a single page time /min
Previous generation modeling platform	6823	13.65
Visual application topology modeling platform	1344	2.69

projected backward. After repeated matching, the 3D point cloud of the object and the attitude of the camera are obtained. The projection of R the three images is $r_1, r_2, r_2^S G r_1 = 0$. The geometric limits of the poles are satisfied. The calculation is carried out with G matrix. Finally, the matrix of the internal and external parameters of the camera is obtained [15]. Combined with the knowledge of triangulation, it can reverse the three-dimensional coordinates of point R . After obtaining the original projection matrix, the paper continues to add a new projection matrix method for repeated operations. The 3D coordinates and projection matrix are obtained by minimizing the equation of (4.1):

$$\min_{C_i, S_i, X_j} \sum_{i=1}^2 \sum_j \|r_{ij} - A[C_i | S_i] R_j\|^2 \quad (4.1)$$

Two feature points of three-dimensional point R_j of (r_{1j}, r_{2j}) are matched. A is the matrix of the camera's internal parameters. Where $[C_i, S_i]$ is the external parameter of the camera.

First, two cameras with the most feature points in the image are selected as targets; The five-point method (RANSAC) was used to identify the camera parameters. Two cameras observe feature points. The spatial coordinates of the feature points are obtained by trigonometry [16]. The beam current adjustment method is used to optimize it. New cameras are added in turn, and the feature points observed by them are used as the target optimal solution. After adding the above parameters, the overall beam adjustment is completed. This method is repeated until other cameras find no new feature points. Some optimizations have been made for speed and robustness:

- 1) The singularity with high projection error is removed each time the optimization is performed—one more adjustment until there are no more singularities.
- 2) Initialize multiple cameras simultaneously. First, add a camera with λ maximum corresponding points. Add at least one feature point that corresponds to 0.75λ .

4.2. Poisson reconstruction. Poisson reconstruction is based on the fact that the equivalent function of the indicator surface reconstructs the points in the point cloud model. It is an implicit function method. This paper transforms the surface reconstruction problem of directed point sets into a spatial Poisson problem. Set the point set in the point cloud as a sample set $l \in L$. Each sample contains a point and an inward average vector. Assume the set of points is on the model's surface [17]. An approximate representation of the model is obtained by estimating the indicator function of the model. The seamless triangular approximation to the model surface is realized by reconstructing the contour surface. The reconstruction program is divided into:

Step 1 is the definition of the octree. Octree is a kind of data structure used to represent the three-dimensional information of objects in space [18]. An octree structure based on a point set L is proposed. The maximum value of an octree is Z . Every node in an octree is P . Set the function G_P to represent the function for each node. $P.B$ stands for the middle node P . $P.E$ represents the width of a node P . v stands for a subject. The extension of G_P is

$$G_P(v) = G \left(\frac{v - P.B}{P.E} \right) \frac{1}{P.E^3} \quad (4.2)$$

In order to make U can be expressed by the linear sum of node functions, the basis function of G is filtered by n times envelope. When the C value increases, the properties are similar to Gaussian filters.

Step 2 is the calculation of the vector field. The approximation of the functional gradient magnetic field of

this index of the child node is calculated by the formula (4.3):

$$U(v) = \sum_{l \in L} \sum_{P \in N_{gbrZ}(l)} \varepsilon_{P,L} G_P(v) l.N \quad (4.3)$$

$N_{gbrZ}(l)$ represents the 8 nodes closest to the sampling point $l.r$ and Z . Where $\varepsilon_{P,L}$ is the weight of third-order linear interpolation. $l.N$ represents an average vector. The vector field U is generated by this method.

Step 3 is the solution to Poisson's equation. Use the vector field U obtained in (3). The index function ρ of the surface can be obtained by the inverse solution of Poisson's equation. The problem is solved in detail by using the Laplacian iterative matrix.

Step 4 is the construction of the equivalent height surface. The step of surface reconstruction is essentially to extract the surface [19]. The position of the sampling point must be estimated and averaged to obtain the surface ∂M . The equivalent surface is derived by formula (4.4) and formula (4.5):

$$\partial M = \{v \in C^3 | \rho(v) = c\} \quad (4.4)$$

$$c = \frac{1}{|L|} \sum_{l \in L} (l.r) \quad (4.5)$$

$|L|$ is how many points there are in a set of points.

5. Experimental design.

5.1. Experimental Data. The measured data test the performance of the software. C++ writes the visualization program of 3D reconstruction. The operating system is Windows 2010. The processor is an Intel i5—speed 7200r/min. In the image acquisition process, this paper simulates the Angle of image acquisition between satellites. Using mobile phones to get images of the lunar probe [20]. In this paper, the image data of the lunar rover are obtained continuously at a certain Angle, and the image data is input into the software platform.

5.2. Result Analysis. Use a ground-based application to transmit high - and low-density reconfiguration commands to a cloud application on a satellite. The resulting 3D reconstruction file is stored in the PLY format. The 3D reconstruction results are displayed in mobile phones and PCS applications. The results of sparse, dense, and Poisson reconstruction of point clouds are demonstrated by MeshLab [21]. Figure 5.1 shows extracting feature point information from non-collaborative objects in 3D reconstruction processing.

The effects of different numbers of experimental images on the reconstruction results were studied. The paper selected 10, 15, and 20 images as the result of the 3D reconstruction (Figure 5.2). When the number of images is 10, the result of 3D reconstruction is relatively poor. The results of 3D reconstruction were better in the case of 15 and 20 photos. And there are more and more photos, and they take longer and longer. The ten photos were restored for a total of about 17 minutes. When the number of images is 15, the reconstruction time is about 30 minutes. When the number of images is 20, the reconstruction time is about 40 minutes. It was reconstructed in 3D with 15 images [22]. It can also be seen from Figure 5.2 that dense point cloud reconstruction has the disadvantages of poor visualization and sparse generated point cloud. To get better display results, intensive reconstruction needs to be further improved.

The paper selected 15 images for 3D reconstruction. The Poisson reconstruction method is used for further optimization based on the reconstruction effect shown in Figure 5.2. The defects in the reconstruction process of the original dense point cloud can be effectively remedied by grid processing. Form a unified and compact surface. The results of the refactoring are shown in Figure 5.3. Through comparative analysis, it can be found that the software system completely restores the structure of the lunar probe. This means that the reconstruction is working very well.

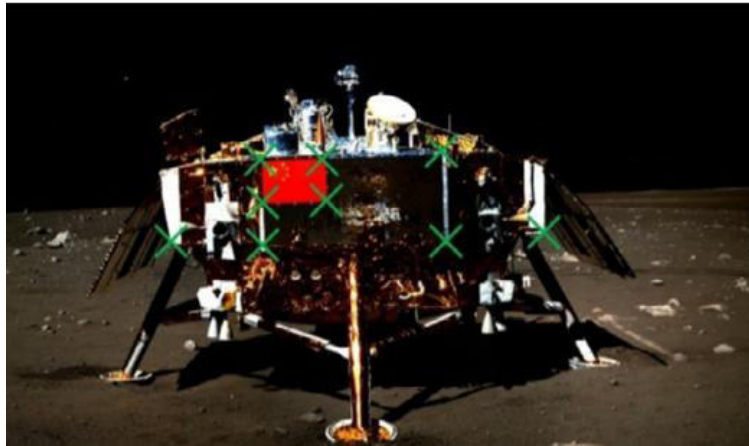


Fig. 5.1: Feature points extracted from the image.

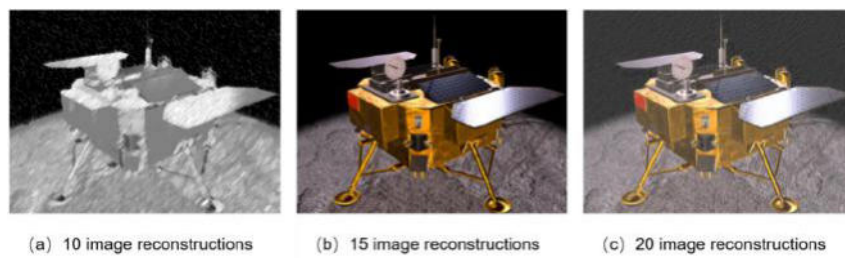


Fig. 5.2: Reconstruction results of dense point cloud.



Fig. 5.3: Poisson reconstruction results.

6. Conclusion. This paper mainly studies the visual topology modeling method of space missions and analyzes and compares the two feasible methods of the current technical route. It provides a new, extensible framework for developing the spatial visualization topology model. This paper introduces a space command display software development scheme on the QtUiLoader platform. The development of the system is easy, and the development period is short. This algorithm is used in space command display software to complete the visualization of the space control interface and the creation of a topological structure diagram. The system completes the feature point extraction, matching and camera position calculation of non-cooperative object images based on the satellite-borne optical camera. A solution model is obtained based on a sparse point array and camera coordinates. It can solve the problem of vector relationship between satellite and non-cooperative object. The system can achieve accurate 3D reconstruction of non-cooperative objects, which meets the requirements of human eye observation and capture. This project provides the theoretical basis and technical support for developing the spatial visualization topology model. However, further work still needs to be carried out to realize human-computer interaction in the system and organically combine the visual topology model with the commercial system simulation.

Acknowledgments. Guangdong Provincial Science and Technology Innovation Strategy Special Fund Project (pdjh2023b0984); Scientific Research Project of the Science and Technology Department of Jingchu Institute of Technology(YB202319). General Science and Technology Plan Project of Jingmen Science and Technology Bureau(2023YFYB085).

REFERENCES

- [1] Gui, G., Zhou, Z., Wang, J., Liu, F., & Sun, J. (2020). Machine learning aided air traffic flow analysis based on aviation big data. *IEEE Transactions on Vehicular Technology*, 69(5), 4817-4826.
- [2] Qiu, R., Hou, S., Chen, X., & Meng, Z. (2021). Green aviation industry sustainable development towards an integrated support system. *Business Strategy and the Environment*, 30(5), 2441-2452.
- [3] Meister, P., Miller, J., Wang, K., Dorneich, M. C., Winer, E., Brown, L. J., & Whitehurst, G. (2022). Designing three-dimensional augmented reality weather visualizations to enhance general aviation weather education. *IEEE Transactions on Professional Communication*, 65(2), 321-336.
- [4] Ayala, R., Ayala Hernández, D., Sellés Vidal, L., & Ruiz Cortés, D. (2021). openSkies-Integration of Aviation Data into the R Ecosystem. *The R Journal*, 13 (2), 590-599.
- [5] Mao, R., Li, G., Hildre, H. P., & Zhang, H. (2021). A survey of eye tracking in automobile and aviation studies: Implications for eye-tracking studies in marine operations. *IEEE Transactions on Human-Machine Systems*, 51(2), 87-98.
- [6] Li, S., Zheng, P., & Zheng, L. (2020). An AR-assisted deep learning-based approach for automatic inspection of aviation connectors. *IEEE Transactions on Industrial Informatics*, 17(3), 1721-1731.
- [7] Puranik, T. G., & Mavris, D. N. (2020). Identification of instantaneous anomalies in general aviation operations using energy metrics. *Journal of Aerospace Information Systems*, 17(1), 51-65.
- [8] Kanavos, A., Kounellis, F., Iliadis, L., & Makris, C. (2021). Deep learning models for forecasting aviation demand time series. *Neural Computing and Applications*, 33(23), 16329-16343.
- [9] Memarzadeh, M., Matthews, B., & Templin, T. (2022). Multiclass Anomaly Detection in Flight Data Using Semi-Supervised Explainable Deep Learning Model. *Journal of Aerospace Information Systems*, 19(2), 83-97.
- [10] Sun, J., Gui, G., Sari, H., Gacanin, H., & Adachi, F. (2020). Aviation data lake: Using side information to enhance future air-ground vehicle networks. *IEEE Vehicular Technology Magazine*, 16(1), 40-48.
- [11] Elakramine, F., Jaradat, R., Hossain, N. U. I., Banghart, M., Kerr, C., & El Amrani, S. (2021). Applying systems modeling language in an aviation maintenance system. *IEEE Transactions on Engineering Management*, 69(6), 4006-4018.
- [12] Shome, S., & Verma, S. (2020). Financial distress in Indian aviation industry: Investigation using bankruptcy prediction models. *Eurasian Journal of Business and Economics*, 13(25), 91-109.
- [13] Kim, G., & Sterkenburg, R. (2021). Investigating the effects aviation fluids have on the flatwise compressive strength of Nomex® honeycomb core material. *Journal of Sandwich Structures & Materials*, 23(1), 365-382.
- [14] WANG, S., CHEN, H., DING, L., SUI, H., & DING, J. (2023). GAN-SR Anomaly Detection Model Based on Imbalanced Data. *IEICE TRANSACTIONS on Information and Systems*, 106(7), 1209-1218.
- [15] Puranik, T., Harrison, E., Chakraborty, I., & Mavris, D. (2020). Aircraft performance model calibration and validation for general aviation safety analysis. *Journal of Aircraft*, 57(4), 678-688.
- [16] Babae, M., Gheidar-Kheljani, J., Khazae, M., & Karbasian, M. (2021). Prediction of Failure Time and Remaining Useful Life in Aviation Systems: Predictors, models, and challenges. *International Journal of Reliability, Risk and Safety: Theory and Application*, 4(2), 97-106.
- [17] Avci, C., Tekinerdogan, B., & Athanasiadis, I. N. (2020). Software architectures for big data: a systematic literature review. *Big Data Analytics*, 5(1), 1-53.
- [18] Walia, S., Sharma, D., & Mathur, A. (2021). The impact of service quality on passenger satisfaction and loyalty in the Indian aviation industry. *International Journal of Hospitality and Tourism Systems*, 14(2), 136-143.

- [19] Jiang, Y., Niu, S., Zhang, K., Chen, B., Xu, C., Liu, D., & Song, H. (2021). Spatial-temporal graph data mining for iot-enabled air mobility prediction. *IEEE Internet of Things Journal*, 9(12), 9232-9240.
- [20] Gogalniceanu, P., Calder, F., Callaghan, C., Sevdalis, N., & Mamode, N. (2021). Surgeons are not pilots: is the aviation safety paradigm relevant to modern surgical practice?. *Journal of Surgical Education*, 78(5), 1393-1399.
- [21] AKPINAR, M. T., HIZIROĞLU, K., & CODAL, K. S. (2023). From Descriptive to Prescriptive Analytics: Turkish Airlines Case Study. *Adam Academy Journal of Social Sciences*, 13(1), 99-125.
- [22] Lee, B., Brown, D., Lee, B., Hurter, C., Drucker, S., & Dwyer, T. (2020). Data visceralization: Enabling deeper understanding of data using virtual reality. *IEEE Transactions on Visualization and Computer Graphics*, 27(2), 1095-1105.

Edited by: Zhigao Zheng

Special Issue on: Graph Powered Big Aerospace Data Processing

Received: Jul 18, 2023

Accepted: Aug 25, 2023